Forty-photon-per-pulse spectral phase retrieval by shaper-assisted modified interferometric field autocorrelation

Chen-Shao Hsu, Hsin-Chien Chiang, Hsiu-Po Chuang, Chen-Bin Huang, and Shang-Da Yang*

Institute of Photonics Technologies, National Tsing Hua University, Hsinchu 30013, Taiwan
**Corresponding author: shangda@ee.nthu.edu.tw*

Received January 28, 2011; revised June 1, 2011; accepted June 10, 2011;
posted June 14, 2011 (Doc. ID 141899); published July 11, 2011

We retrieve the spectral phase of 400 fs pulses at 1560 nm with 5.2 aJ coupled pulse energy (40 photons) by the modified interferometric field autocorrelation method, using a pulse shaper and a 5 cm long periodically poled lithium niobate waveguide. The carrier-envelope phase control of the shaper can reduce the fringe density of the interferometric trace and permits longer lock-in time constants, achieving a sensitivity of 2.7×10^{-9} mW^2 (40 times better than the previous record for self-referenced nonlinear pulse measurement). The high stability of the pulse shaper allows for accurate and reproducible measurements of complicated spectral phases.

OCIS codes: 320.7100, 190.7110, 120.3180.

Characterization of the spectral phase of ultrashort pulses in the picosecond to attosecond regimes plays a pivotal role in a variety of applications [1–3]. On the other hand, the pulse shaper has been widely used to produce optical and radio frequency waveforms with extremely high complexity [4]. The marriage between the pulse shaping and the pulse measurement techniques has received great attention in recent years and enabled a series of shaper-assisted pulse measurement schemes, such as time-domain interferometry [5], multiphoton intrapulse interference phase scan (MIIPS) [6], four-wave mixing autocorrelation [7], spectral shear interferometry for direct electric field reconstruction (SPIDER) [8], sonogram [9], intensity autocorrelation, frequency resolving optical gating (FROG), and spectrally and temporally resolved up-conversion techniques[10]. In these applications, the pulse shaper is used to implement beam splitting, delay scanning, tunable filtering, or generation of chirped reference pulse, which are typically carried out by bulk or fiber optics. As a result, they are particularly advantageous in terms of measuring ultrabroadband (more than one octave) signals [7], all-in-one integration of pulse manipulation and measurement, elimination of a reference beam and additional dispersion, as well as measuring the pulse at the point of experiment (such as the focal point of a high numerical aperture microscope objective) [8]. In practice, a pulse shaper might be most valued for signal characterizations because of its carrier-envelope phase (CEP) control functionality, which is absent for any other optical component. CEP control has been proposed to mitigate the phase-cycle slip errors in SPIDER [8] and demonstrated to reduce the average fringe density of interferometric data traces [10]. However, the former has not been experimentally verified, and the latter only exhibited a limited accuracy when the fringe density reduction was coupled with a weak pulse chirp.

We have proposed and experimentally demonstrated the modified interferometric field autocorrelation (MIFA) method to analytically measure the spectral amplitude and phase of nearly transform-limited and slightly modulated pulses with record high sensitivity by a fiber-based setup and a reference CW laser (for fringe correction) [11,12]. The setup only consisted of a standard collinear Michelson interferometer, a thick nonlinear crystal, and a slow point detector, without using any reference pulse, spectrograph, and detector array. The same method also succeeded in measuring 8 fs pulses at 600 nm by using 300 mm thick lithium triborate crystals [13]. In this Letter, we showed that the unique stability and CEP control of a pulse shaper are particularly useful for pulse measurement techniques relying on interferometric delay scanning. Accurate and reproducible measurements of complicated spectral phases were experimentally demonstrated by a MIFA setup composed of a Fourier pulse shaper and a 5 cm long unchirped periodically poled lithium niobate (PPLN) waveguide. The longer lock-in time constant, due to the reduced fringe density, achieves an unprecedented measurement sensitivity of 2.7×10^{-9} mW^2, improving on the previous records of FROG [12] and MIFA [12] by 800 and 40 times, respectively. The shaper-assisted MIFA is free of external reference pulse, precise calibration, and stringent requirement of the spectrometer resolution [8]. It does not need iterative measurements [6] or data inversion [9,10] and is immune to the limit of a finite phase-matching bandwidth. These advantages, along with the simple configuration and high sensitivity, make it promising in simultaneous measurement and manipulation of low-power femtosecond and even subfemtosecond optical pulses.

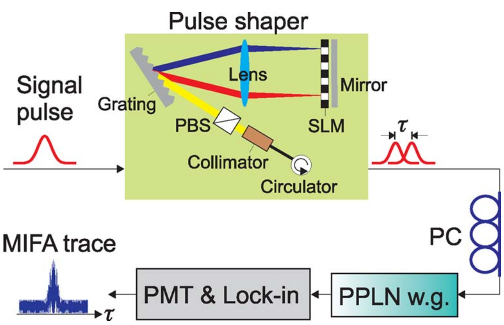

Fig. 1. (Color online) Experimental setup. PBS, polarization beam splitter; SLM, spatial light modulator; PC, polarization controller; PMT, photomultiplier tube.

Figure 1 shows the setup of the shaper-assisted MIFA experiments. The signal pulse train (50 MHz, 400 fs, 1560 nm) coming from a passively mode-locked Er-doped fiber laser was sent into a homemade reflective pulse shaper with ~5 dB back-to-back loss, 15.5 GHz spectral resolution, and 80 nm (1520–1600 nm) spectral window. A detailed shaper setup is described in [2]. The pulse replicas with variable delay and desired CEP were produced by the pulse shaper via a complex transfer function of [10]:

$$M(f) = \frac{1}{2}\{1 + e^{-j2\pi[f-(1-\beta)\times f_0]\tau}\}, \tag{1}$$

where $\beta (0 < \beta < 1)$ represents the carrier frequency reduction factor. The signal pulse replicas from the pulse shaper were coupled into a 5 cm long PPLN waveguide for second-harmonic generation, where the phase-matching bandwidth (FWHM) was only 50 GHz (≈3% of the signal bandwidth Δ_f). The average second-harmonic power at each delay was detected by a photomultiplier tube and a lock-in amplifier. To retrieve the spectral phase, the peak phase-matching wavelengths were set to 780.1 nm (45 °C) and 780.6 nm (51.5 °C) when acquiring the two MIFA traces, respectively. As explained in [11,12], processing the two MIFA traces due to thick nonlinear crystals with peak phase-matching frequencies of $2f_0$ and $2(f_0 - \Delta)$ ($f_0 = 192.28$ THz, $\Delta = 0.12$ THz in the experiments) produces two "even" spectral phase functions $\psi_{e1}(f) = [\psi(f) + \psi(-f)]/2$ and $\psi_{e2}(f) = [\psi(f) + \psi(-f - 2\Delta)]/2$, from which the spectral phase $\psi(f)$ of the unknown pulse can be retrieved by a recursive relation:

$$\psi(f - 2\Delta) - \psi(f) = 2[\psi_{e2}(f - 2\Delta) - \psi_{e1}(f)]. \tag{2}$$

Figure 2 illustrates the experimentally measured quadratic spectral phase coefficient c_2 versus the carrier frequency reduction factor β (achieved by the CEP control), where the spectral phase is approximated by $\psi(f) \approx c_2 f^2$. The results show that the MIFA measurement remains accurate until the equivalent carrier frequency is about $0.016 f_0$ or twice the signal bandwidth Δ_f. The standard deviation of six measurements of c_2 at $\beta = 0.04$ is only $0.0254\ \mathrm{ps}^2$, equivalent to the dispersion caused by a 5.6 cm long single mode fiber. As a result, we chose $\beta = 0.038$ and a delay step size of 26.7 fs (better than the Nyquist criterion of $(4\beta f_0)^{-1}$) to carry out the experiments.

Figure 3 illustrates the retrieved spectral phase profiles at fundamental average powers (coupled into the PPLN waveguide) of 0.8 μW (solid curve) and 0.26 nW (open circles), respectively. The two phase curves are nearly indistinguishable even in the presence of 35 dB input power difference. The 0.26 nW average power is equivalent to 10 μW peak power, 5.2 aJ pulse energy, and 40 photons per pulse. These numbers correspond to an unprecedented sensitivity of $2.7 \times 10^{-9}\ \mathrm{mW}^2$, improving on the previous records of FROG [14] and interferometer-based MIFA [12] by 800 and 40 times, respectively. Compared with the system in [12], the current setup does not need a CW reference laser and permits a much longer lock-in time constant (50 ms, versus 0.64 ms in [12]) because the pulse shaper can provide accurate delay scanning and dramatically reduce the fringe density via CEP control. Acquiring one MIFA trace with a 10 ps delay window took 2 min, primarily limited by the update speed of the spatial light modulator pixels (~300 ms).

In addition to the high sensitivity, we also demonstrated that the shaper-assisted MIFA method is able to retrieve complicated spectral phase profiles. We used the pulse shaper to fully compensate for the residual spectral phase of the signal pulse and added three types of additional phase modulations $\psi^{(i)}_{\mathrm{mod}}(f)$ $(i = 1, 2, 3)$ for verification. The applied and retrieved spectral phase functions are shown as solid curves and open circles in Fig. 4, respectively. In Fig. 4(a), a cubic phase of $\psi^{(1)}_{\mathrm{mod}}(f) = 2\ \mathrm{ps}^3 \cdot f^3$ was added and accurately retrieved by the shaper-assisted MIFA method. The corresponding temporal intensity exhibits six side lobes ahead of the main lobe, which is a signature of strong cubic phase modulation. Figure 4(b) illustrates that a square phase of 1π indention

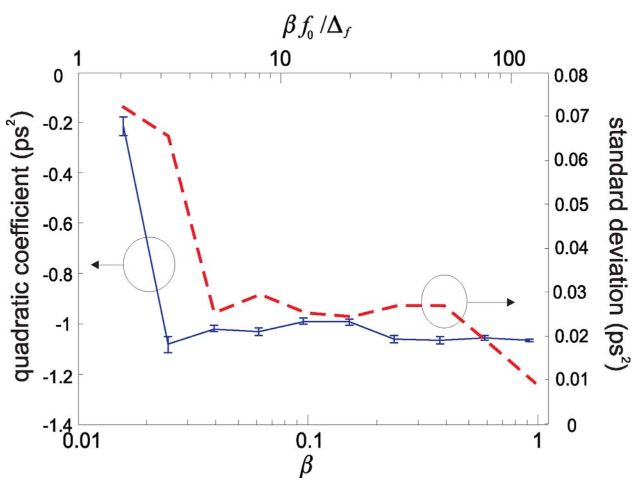

Fig. 2. (Color online) Quadratic spectral phase coefficient measured by the shaper-assisted MIFA at different β values (solid curves), where the full length of each error bar represents the standard deviation of six measurements. The standard deviation is independently shown (dashed curve).

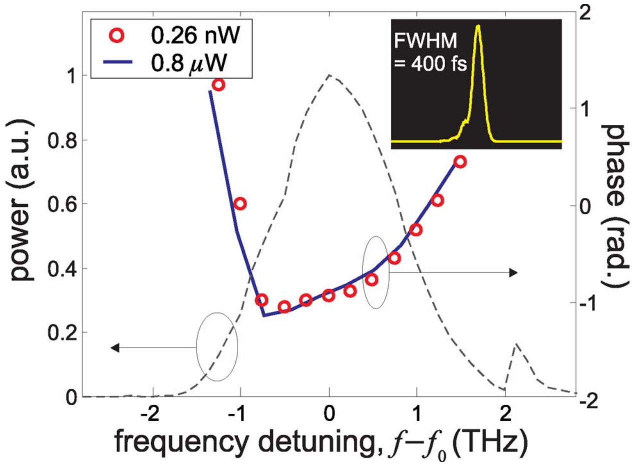

Fig. 3. (Color online) Spectral phase profiles retrieved by the shaper-assisted MIFA at $\beta = 0.038$ and input average powers of 0.8 μW (solid curve) and 0.26 nW (open circles), respectively. The inset shows the temporal intensity arising from the retrieved spectral phase and the power spectrum measured by OSA (dashed curve).

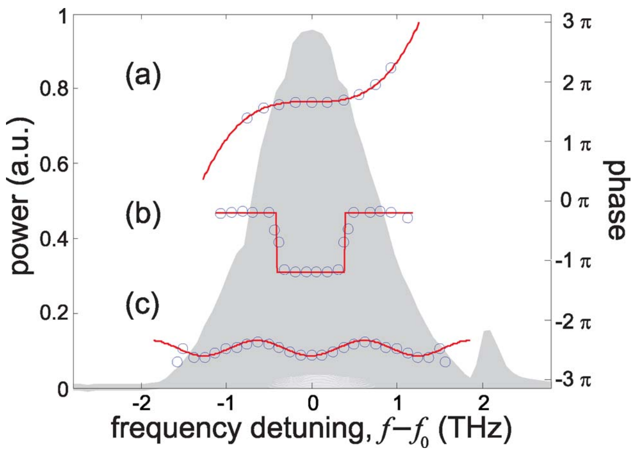

Fig. 4. (Color online) Experimentally retrieved spectral phases (open circles) corresponding to the application of: (a) cubic phase, (b) square phase, and (c) sinusoidal phase (solid curve), respectively. For comparison, the signal power spectrum is indicated as the gray shaded area.

depth, i.e., $\psi^{(2)}_{\mathrm{mod}}(f) = \{-\pi, \quad \text{if } |f| < 0.4\,\mathrm{THz}; 0, \text{otherwise}\}$, can be successfully retrieved. Note that such a large indention depth can lead to disruptions in the SPIDER interferograms and systematic errors in the phase reconstruction [8], while MIFA can still retrieve it with high fidelity. In Fig. 4(c), a sinusoidal phase modulation of the form $\psi^{(3)}_{\mathrm{mod}}(f) = -K\cos(2\pi\tau_m f)$ was tested, where $K = 0.13\pi$, $\tau_m = 0.8\,\mathrm{ps}$, respectively. The sinusoidal phases are of practical importance in single-pulse coherent anti-Stokes Raman spectroscopy [1] and MIIPS measurement [6]. The spectral phase curve measured by the shaper-assisted MIFA method (open circles) agrees well with the applied one (solid) over a wide spectral range corresponding to ~92% of the total power (spectral area). These experimental results confirm the feasibility of our approach in measuring complicated spectral phases and creating the desired pulse shapes at the point of experiment.

We have experimentally demonstrated that the shaper-assisted MIFA method using long PPLN waveguides can analytically measure complicated spectral phases of ultraweak, ultrashort pulses with high accuracy, reproducibility, and sensitivity. The setup only consists of a Fourier pulse shaper, a thick nonlinear crystal, and a slow point detector, without using any reference light, spectrograph, and detector array. The achieved sensitivity is $2.7 \times 10^{-9}\,\mathrm{mW}^2$, about 40 times better than the previous record. This scheme can be generalized to interferometric spectrogram measurement, from which multiple data inversion approaches can be used to recover the complex envelope of the unknown pulse with better robustness against measurement noise [15].

Space-time coupling effect [16] is not apparent in our current experiments since our pulse shaper is designed to have a 64 ps time-window with a spot size approximately equal to the liquid crystal pixel dimension. Investigations into space-time coupling might bring new aspects for future optimization and are underway.

The authors gratefully thank Carsten Langrock and Martin. M. Fejer for supporting the PPLN waveguide.

This work is supported by the National Science Council of Taiwan (NSCT) under grants NSC 97-2221-E-007-028-MY3, NSC 97-2112-M-007-025-MY3, and NSC-99-2120-M-007-010.

References

1. N. Dudovich, D. Oron, and Y. Silberberg, Nature **418**, 512 (2002).
2. H.-P. Chuang and C.-B. Huang, Opt. Express **18**, 24003 (2010).
3. W.-J. Chen, J.-M. Hsieh, S.-W. Huang, H.-Y. Su, C.-J. Lai, T.-T. Tang, C.-H. Lin, C.-K. Lee, R.-P. Pan, C.-L. Pan, and A. H. Kung, Phys. Rev. Lett. **100**, 163906 (2008).
4. S. Cundiff and A. M. Weiner, Nat. Photon. **4**, 760 (2010).
5. C. Ventalon, J. M. Fraser, and M. Joffre, Opt. Lett. **28**, 1826 (2003).
6. Y. Coello, V. V. Lozovoy, T. C. Gunaratne, B. W. Xu, I. Borukhovich, C. H. Tseng, T. Weinacht, and M. Dantus, J. Opt. Soc. Am. B **25**, A140 (2008).
7. H.-S. Chan, Z.-M. Hsieh, W.-H. Liang, A. H. Kung, C.-K. Lee, C.-J. Lai, R.-P. Pan, and L.-H. Peng, Science **331**, 1165 (2011).
8. B. von Vacano, T. Buckup, and M. Motzkus, J. Opt. Soc. Am. B **24**, 1091 (2007).
9. J. Möhring, T. Buckup, and M. Motzkus, Opt. Lett. **35**, 3916 (2010).
10. A. Galler and T. Feurer, Appl. Phys. B **90**, 427 (2008).
11. S.-D. Yang, C.-S. Hsu, S.-L. Lin, H. Miao, C.-B. Huang, and A. M. Weiner, Opt. Express **16**, 20617 (2008).
12. S.-D. Yang, C.-S. Hsu, S.-L. Lin, Y.-S. Lin, C. Langrock, and M. M. Fejer, Opt. Lett. **34**, 3065 (2009).
13. C.-S. Hsu, Y.-H. Lee, A. Yabushita, T. Kobayashi, and S.-D. Yang, Opt. Lett. **36**, 2041 (2011).
14. H. Miao, S.-D. Yang, C. Langrock, R. V. Roussev, M. M. Fejer, and A. M. Weiner, J. Opt. Soc. Am. B **25**, A41 (2008).
15. L.-F. Yang, S.-L. Lin, and S.-D. Yang, Opt. Express **18**, 6877 (2010).
16. M. M. Wefers and K. A. Nelson, IEEE J. Quantum Electron. **32**, 161 (1996).